Chapter 62
Study of Effects of Grouting Defects on the Seismic Performance of Precast Concrete Shear Walls with Different Structural Characteristics

Dong Cao, Pan Zuanfeng, and Bin Zeng

Abstract Precast concrete structure is the trend of intelligent construction of green buildings in the future. Grouting sleeve connection has the advantages of convenient construction and connection performance equivalent to cast-in-place, and is widely used in steel bar connection of precast concrete structures. Controlling the compactness of sleeve grouting is the key to ensure the construction quality and structural reliability of precast structures. In order to analyze the influence of grouting defects on the seismic performance of assembled shear walls, the finite element simulation was carried out based on OpenSees with the location of grouting defects, the length of defects and the number of grouting defect sleeves as variables. Considering the diversity of the grouting sleeve shear walls, the sensitivity of the characteristic parameters such as sleeve spacing and edge constraint area to grouting defects was studied. The results show that the precast concrete shear walls with grouting defects will have different degrees of loss in bearing capacity, energy dissipation capacity and ductility. The bearing capacity and energy dissipation capacity of the shear wall connected by grouting sleeve are greatly affected by grouting defects. The sensitivity of equivalent stiffness and ductility coefficient to grouting defects is lower than that of bearing capacity and energy dissipation capacity. The grouting defects in the embedded column of the shear wall connected by grouting sleeve have a significant effect on the seismic performance.

Keywords Grouting sleeves · Grouting defects · Precast concrete shear walls · Seismic performance

D. Cao · P. Zuanfeng (✉)
College of Civil Engineering, Tongji University, Shanghai 200092, China
e-mail: zfpan@tongji.edu.cn

B. Zeng
Central Research Institute of Building and Construction of MCC Group, Beijing 100088, China

S. Li (ed.), *Computational and Experimental Simulations in Engineering*, Mechanisms and Machine Science 143,
https://doi.org/10.1007/978-3-031-42515-8_62

62.1 Introduction

Precast concrete structure system is an important part of intelligent construction. It has the advantages of good product quality, short construction period and high degree of modernization. Precast concrete shear wall structure is widely used in residential projects. Grouting sleeve undertakes the important task of connecting precast shear wall and vertical reinforcement [1]. Grouting sleeve connection realizes the connection of longitudinal discontinuous reinforcement through the bonding force of high strength grouting material [2]. The method of grouting sleeve connection belongs to wet connection technology, and some scholars have studied the effectiveness of dry connection method [3–6]. Because in the process of prefabricated shear wall manufacturing, the grouting sleeve is embedded inside the shear wall. Therefore, the engineering concealment problem of grouting compactness is one of the difficulties in the research of assembly industry. At present, the research on grouting sleeve mainly includes grouting defect detection, grouting sleeve bonding force, and the influence of grouting defects on the seismic performance of components [1, 7–9].

For the detection of grouting sleeve compactness, Li et al. [8] used acoustic emission method to detect the compactness of grouting sleeve. The results show that the amplitude and frequency of acoustic emission signal of grouting-compact sleeve are greater than that of grouting-defective sleeve. Lu [9] combined acoustic emission and ultrasonic detection methods to evaluate the damage of grouting-defective sleeve. However, at present, there is no mature and effective detection method that can comprehensively and quantitatively detect the grouting quality of steel connection sleeve.

Wang [10] studied the grouting sleeve from multiple perspectives, including insufficient strength of grouting materials, insufficient anchorage length, and low temperature environment. At the same time, the safety performance of different defect casings in winter environment was evaluated. Zheng [11] carried out uniaxial tensile test and cyclic load test on the sleeve with vertical grouting defects. The results show that the failure mode and tensile capacity of sleeve are related to the anchorage length of steel bar. The displacement deformation of grouting-defective sleeve is obviously higher than that of grouting-compact sleeve. Xiao [1] carried out cyclic loading tests on shear walls with grouting defects. The test results show that the bearing capacity of the shear wall with grouting defects is significantly lower than that of the shear wall with dense grouting. Gu [12] studied the reinforcement of shear wall with grouting defects. The results show that the crack propagation of shear wall reinforced by steel plate is effectively limited, and the damage degree is obviously reduced.

In this paper, the prefabricated shear wall with grouting defects is taken as the object to study the influence of sleeve grouting defects on the seismic performance of shear wall members. The influence of different grouting defects on the load–displacement hysteresis curve, bearing capacity, displacement ductility and energy dissipation capacity of prefabricated concrete shear wall is analyzed. The refined numerical model of grouting-defective prefabricated concrete shear wall is established. Through parameter analysis, the variation law of seismic performance of grouting-defective prefabricated concrete shear wall is systematically revealed.

62.2 Finite Element Model

62.2.1 Material Constitutive

The steel bar adopts Steel02 material in OpenSees, and the isotropic strengthening of the steel bar under repeated load can be considered. The Concrete01 model is selected for the concrete material model. When defining concrete constitutive, it is necessary to clarify the peak compressive strength, peak compressive strain, ultimate compressive strength and ultimate compressive strain. For the definition of concrete material in stirrup confined core area, Mander stirrup-confined concrete constitutive is selected [13].

62.2.2 Node Settings

The overall node division of the shear wall is shown in Fig. 62.1a. Although the accuracy of the model can be improved by increasing the number of shear wall divisions, the difference in accuracy is very small after the division to a certain level, and the calculation time will be increased [14]. The wet connection of the vertical reinforcement of the shear wall adopts a full-size grouting sleeve. In the study, only the bond anchorage defects in the upper half of the slurry outlet are considered. The sleeve grouting shear wall adopts NLDKGQ layered shell element to establish the wall body, and the concealed column of the shear wall is modeled by fiber model.

62.2.3 Grouting Defect Simulation

The experimental results of [2, 15] show that the influence of grouting defects on the mechanical properties of sleeve is mainly the reduction of bearing capacity and the reduction of ductility. The sleeve with grouting defects can be simulated by bond strength reduction [3]. The specification JGJ355-2015 [16] stipulates the limit value of the anchorage length of the grouting material, which requires that the diameter of the vertical steel bar is not less than 12 mm, and the anchorage length is greater than 8 times than the diameter of the steel bar (*d* represents the diameter of the steel bar). In reference [11], the influence of grouting defects on the pull-out bearing capacity of full-size grouting sleeve was studied. For the sleeve with 4 *d* vertical

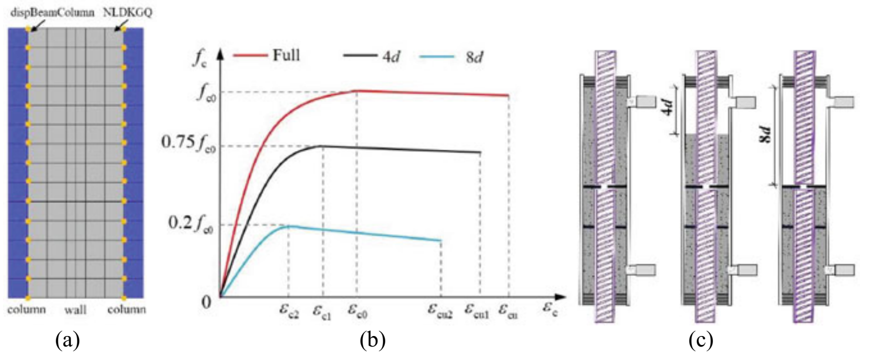

Fig. 62.1 Grouting sleeve shear wall node setting and defect setting method: **a** node distribution, **b** definition of bearing capacity reduction, **c** grouting defect setting

anchorage length damage (defined as state D1), the reduction coefficient of strength bearing capacity of sleeve connection is 0.75. For sleeves with vertical grouting defect length of 8*d* (defined as state D2), the comprehensive value of the strength bearing capacity reduction coefficient is 0.2. The reduction relationship and grouting damage of the bearing capacity of the grouting sleeve are shown in Fig. 62.1b and c, respectively.

62.2.4 Method Validation

Reference [1] conducted a comparative study on the influence of grouting defects on the seismic performance of shear walls. It can be found from Fig. 62.2 that the numerical simulation results are close to the experimental results. The comparison between the energy dissipation capacity of the hysteresis curve simulated by Fig. 62.3 and the energy dissipation capacity of the test data shows that the overall trend is still relatively consistent.

62.3 Parametric Analysis

The overall size of the shear wall model is 2.8 × 1.4 × 0.2 m, the aspect ratio is 2, the concrete cube strength is C30, the section of the edge constraint column is 200 × 200 mm, the design axial compression ratio is 0.2, and the vertical reinforcement diameter is 16 mm. From the bottom of the shear wall to the top, horizontal distribution bars with a diameter of 8 mm is arranged along the spacing of 50 mm. The numbering rules of the shear wall are JLQ-I-II-III, where I represents the design characteristics of the shear wall; II represents the position of the grouting-defective sleeve;

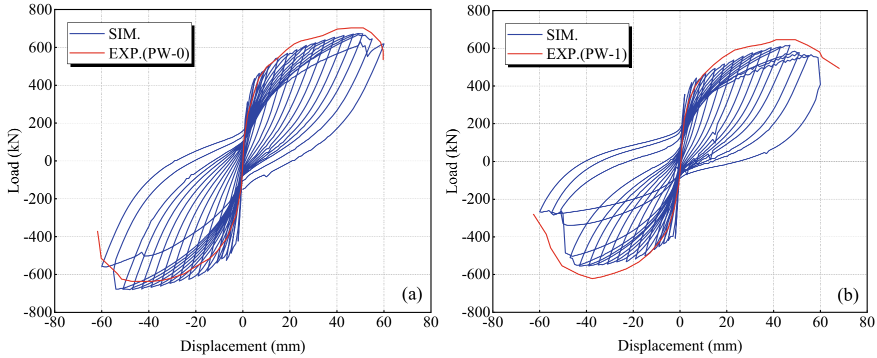

Fig. 62.2 Comparison of hysteresis curves: **a** PW-0, **b** PW-1 [1]

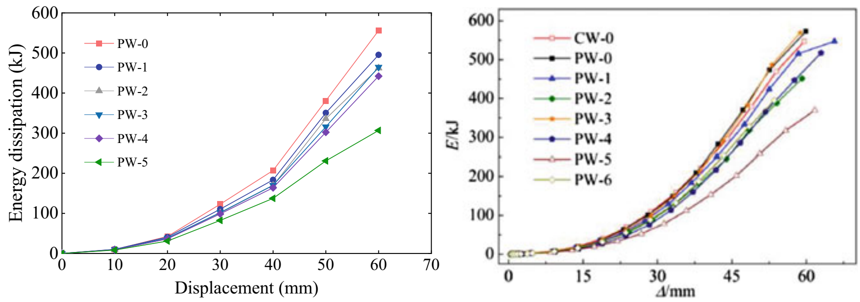

Fig. 62.3 Comparison of energy consumption curves: **a** PW-0, **b** PW-1 [1]

III represents the defect degree of grouting sleeve. The defect sleeve combination is set as Fig. 62.4.

The performance of sleeve grouting connection shear wall structure depends on the design of sleeve grouting connection shear wall components, and the key to the performance of assembled shear wall components lies in the quality of assembled connectors. In order to study the influence of grouting defects on the seismic performance of shear walls with different structural characteristics, the finite element simulation of variable parameter analysis of shear walls is designed. The characteristics of the shear wall are shown in Table 62.1.

62.3.1 Sleeve Spacing

1. *Load–displacement curve.* According to the specification JGJ1-2014 [17], the sleeve spacing of grouting sleeve connecting members should be less than 300 mm. In order to study the sensitivity of sleeve arrangement spacing to

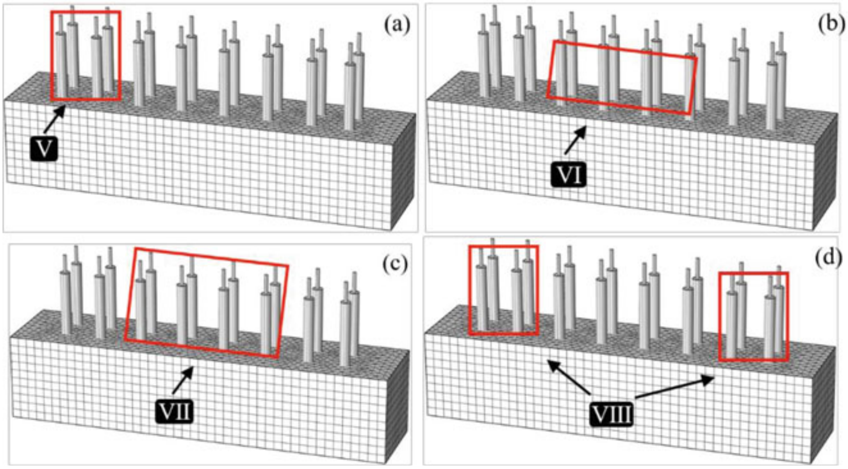

Fig. 62.4 Grouting defect sleeve combination: **a** defect combination V, **b** defect combination VI, **c** defect combination VII, **d** defect combination VIII

Table 62.1 Design parameters of grouting sleeve shear wall

No	Aspect ratio	Sleeve spacing (mm)	Column width (mm)	Strength (MPa)
JLQ-A1	2	150	200	30
JLQ-A2	2	200	200	30
JLQ-B1	2	200	300	30
JLQ-B2	2	200	400	30

grouting defects and the variation of seismic performance, A1 and A2 models of shear wall were set up. Figure 62.5 is the load–displacement curve of shear wall A1 under different grouting defect combinations. It can be directly seen from the figure that the hysteretic curve of the fully grouted shear wall is full and the pinch phenomenon is obvious, while the hysteresis curve of the shear wall A1-V-D2 and A1-VIII-D2 shows a downward trend in the bearing capacity at the key points, and the hysteresis curve is full and weakened.

2. *Ductility and stiffness*. Tables 62.2 and 62.3 are the characteristic values of ductility coefficient of different shear walls under the combination of grouting defects, where D_y is the equivalent yield displacement, F_y is the equivalent yield load, D_p is the peak displacement, F_p is the peak load, D_u is the ultimate displacement, F_u is the ultimate load, and the ductility coefficient $\lambda = D_u / D_y$.

The equivalent yield load F_y, peak load F_p and ultimate load F_u of the shear wall with grouting defects are smaller than those of the grouting-compact shear wall. By comparing and analyzing the bearing capacity and ductility coefficient of grouting-compact shear wall A1-health and A2-health, it can be found that increasing the spacing of sleeve arrangement is beneficial to improve the bearing capacity and

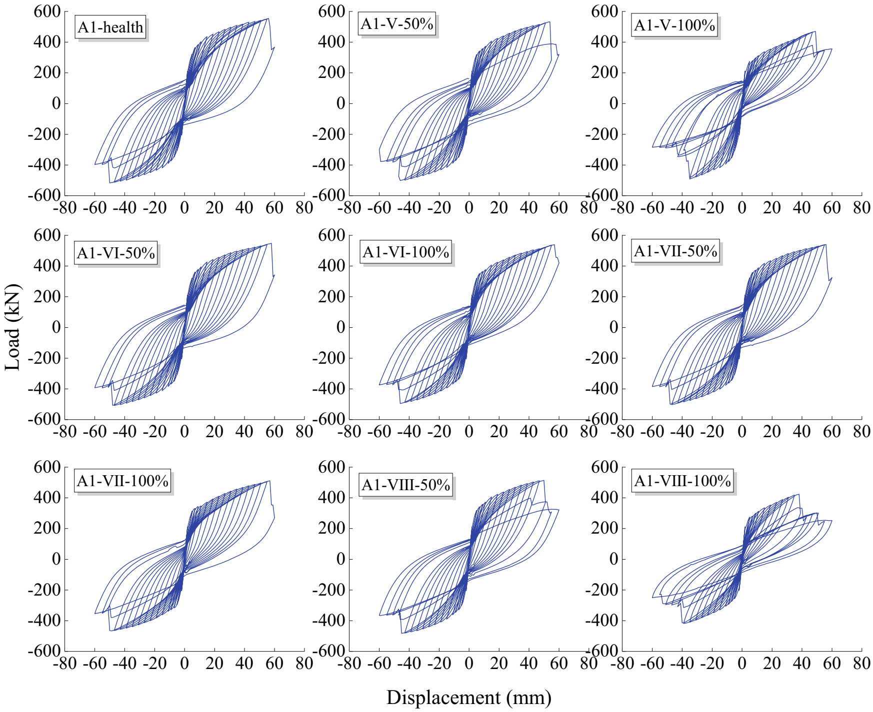

Fig. 62.5 Load–displacement curves of shear wall A1 under different grouting defect combinations

Table 62.2 Ductility coefficient of shear wall A1 under different grouting defect combinations

NO	D_y/mm	F_y/kN	D_p/mm	F_p/kN	D_u/mm	F_u/kN	λ
A1-health	20.4	415.7	55	509.2	57.2	509.2	2.80
A 1-V-D1	20.7	389.1	51	486.4	54.6	413.5	2.64
A1-V-D2	25.8	348.2	55	445.0	55.0	378.3	2.13
A1-VI-D1	19.9	404.0	53	499.6	54.6	424.6	2.74
A1-VI-D2	21.1	390.6	54	488.5	55.1	415.2	2.61
A1-VII-D1	20.6	399.4	54	497.5	55.2	422.8	2.68
A1-VII-D2	21.1	360.0	51	454.4	53.9	386.2	2.55
A1-VIII-D1	19.8	384.1	50	478.1	50.6	406.4	2.55
A1-VIII-D2	18.8	308.6	44	388.9	44.7	330.6	2.38

ductility of grouting sleeve shear wall. However, in cyclic loading, the shear wall with a sleeve spacing of 200 mm yielded before the shear wall with a sleeve spacing of 150 mm.

For the shear wall A1-health, $F_y = 509.2$kN, $F_p = 469.3$kN, $\lambda =$ 2.8. Compared with the shear wall A1-health model, F_y of the shear wall A1-V-D2 model decreased

Table 62.3 Ductility coefficient of shear wall A2 under different grouting defect combinations

NO	D_y/mm	F_y/kN	D_p/mm	F_p/kN	D_u/mm	F_u/kN	λ
A2-health	19.0	453.2	55	550.4	57.2	467.8	3.01
A2-V-D1	20.4	430.4	54	532.5	56.3	452.6	2.76
A2-V-D2	22.0	368.4	49	469.3	55.8	398.9	2.54
A2-VI-D1	20.7	448.9	58	548.7	58.7	466.4	2.84
A2-VI-D2	21.5	434.5	57	539.0	59.0	458.2	2.74
A2-VII-D1	20.2	439.6	56	541.0	57.5	459.9	2.85
A2-VII-D2	22.1	407.5	57	511.0	58.0	434.4	2.62
A2-VIII-D1	18.0	418.8	50	514.5	51.1	437.3	2.84
A2-VIII-D2	15.5	338.1	38	423.8	44.2	360.2	2.86

by 16.2%, F_p decreased by 12.6%, and the ductility coefficient decreased by 23.9%. Compared with the shear wall A2-health model, F_y of the shear wall A2-V-D2 model decreased by 16.2%, F_p decreased by 12.6%, and λ decreased by 23.9%. Comparing the bearing capacity and ductility coefficient of shear wall with different grouting defects, it can be found that the influence of grouting defects on the seismic performance of shear wall is significantly higher than that of wall panel.

Figure 62.6 is the equivalent stiffness curve of shear wall A1 and shear wall A2 under the combination of multiple sleeve grouting defects. From the diagram, it can be found that the grouting defects in the concealed column have the most significant influence on the equivalent stiffness. The maximum decrease rate of equivalent stiffness of shear wall A1 under different grouting defects is 16.8%, and the maximum decrease rate of equivalent stiffness of shear wall A2 is 15.6%.

3. *Cumulative energy dissipation.* The influence of grouting defect combination on the cumulative energy dissipation of shear wall A1 and shear wall A2 is

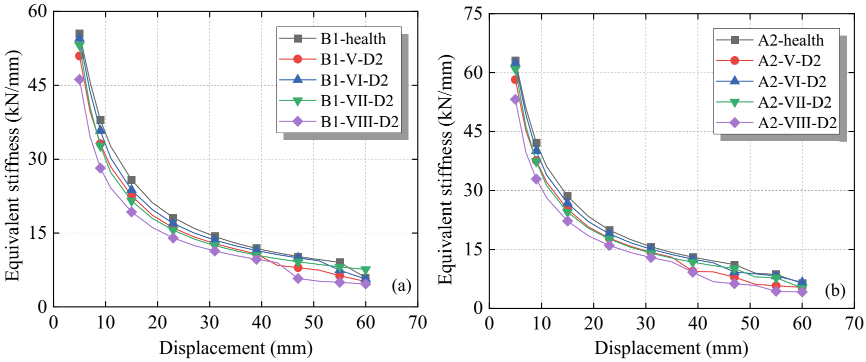

Fig. 62.6 The equivalent stiffness curves of shear wall A1 and A2 under different grouting defect combinations

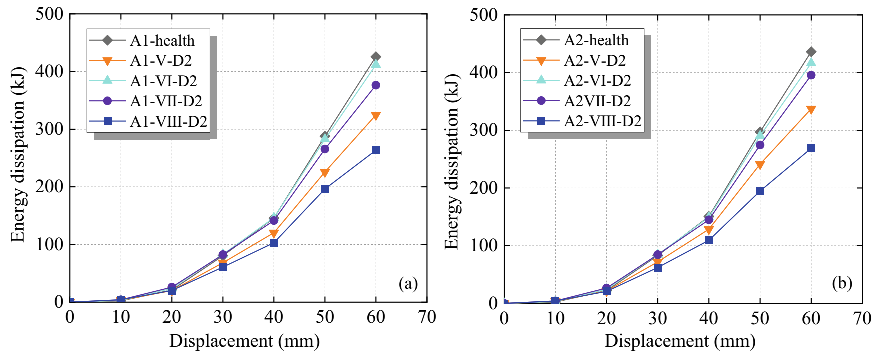

Fig. 62.7 The energy dissipation curves of shear wall A1 and A2 under different grouting defect combinations

further analyzed. It can be seen from Fig. 62.7 that as the degree of grouting defects increased and the grouting-defective sleeve is transferred from the wall panel to the concealed column, and the cumulative dissipation energy curve is continuously reduces. The energy dissipation of shear wall A1 under V-D2, VI-D2, VII-D2 and VIII-D2 defects decreased to 23.7, 3.3, 11.6 and 38.1%, respectively. The energy dissipation of shear wall A2 under V-D2, VI-D2, VII-D2 and VIII-D2 defects decreased to 22.7, 4.5, 9.3 and 38.4%.

62.3.2 Width of Concealed Column

1. *Load–displacement curve*. In order to study the sensitivity of the width change of the edge constraint zone of the shear wall to the grouting defect and the seismic performance, the shear wall B1 and shear wall B2 models were set up. Figure 62.8 shows the load–displacement curves of shear wall B1 and shear wall B2 without grouting defects. It can be seen from the figure that the hysteresis curves of the two models are full, and increasing the length of the edge constraint zone helps to improve the peak bearing capacity of the shear wall.
2. *Ductility and stiffness*. Tables 62.4 and 62.5 are the calculated values of ductility coefficient characteristics of shear wall B1 and B2 under different grouting defect combinations. Comparing and analyzing the grouting-compact shear wall with different width of concealed column, it can be seen that the overall bearing capacity of shear wall is positively correlated with the width of concealed column. The shear wall with larger width of concealed column will yield earlier than the shear wall with smaller width of concealed column under cyclic loading.

From the change of ductility coefficient λ, it can be seen that grouting defects will affect the ductility deformation capacity of shear wall. The ductility coefficient of B1-V-D2 and B2-V-D2 is the lowest of B1 and B2 shear walls. The ductility coefficient of

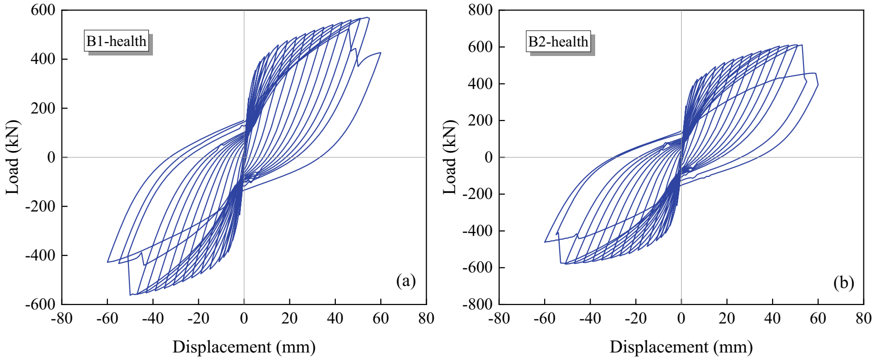

Fig. 62.8 The hysteresis curves of shear wall B1 and B2 without grouting defects

Table 62.4 Ductility coefficient of shear wall B1 under different grouting defect combinations

NO	D_y/mm	F_y/kN	D_p/mm	F_p/kN	D_u/mm	F_u/kN	λ
B1-health	17.9	470.8	54	570.9	56.5	485.2	3.16
B1-V-D1	18.5	446.4	52	549.8	52.5	467.3	2.84
B1-V-D2	21.0	394.8	51	497.5	51.6	422.9	2.46
B1-VI-D1	18.1	464.0	54	566.8	55.5	481.7	3.07
B1-VI-D2	18.4	446.6	54	551.7	54.5	468.9	2.96
B1-VII-D1	17.6	450.9	51	553.1	53.7	470.2	3.05
B1-VII-D2	18.6	414.5	54	519.4	54.7	441.5	2.94
B1-VIII-D1	17.5	437.6	50	537.1	50.6	456.5	2.88
B1-VIII-D2	15.8	366.6	42	457.0	48.5	388.5	3.07

Table 62.5 Ductility coefficient of shear wall B2 under different grouting defect combinations

NO	D_y/mm	F_y/kN	D_p/mm	F_p/kN	D_u/mm	F_u/kN	λ
B2-health	16.5	501.3	50	611.5	53.6	519.8	3.24
B2-V-D1	16.3	484.4	50	593.2	50.5	504.2	3.09
B2-V-D2	19.4	435.3	51	544.0	51.5	462.4	2.65
B2-VI-D1	17.0	493.4	51	605.6	53.0	514.7	3.12
B2-VI-D2	17.2	477.4	51	590.0	54.8	501.5	3.18
B2-VII-D1	16.7	484.0	51	594.6	55.5	505.4	3.32
B2-VII-D2	18.2	457.3	51	572.5	55.8	486.6	3.07
B2-VIII-D1	17.3	470.6	51	581.6	54.0	494.4	3.13
B2-VIII-D2	15.7	402.9	42	506.0	46.7	430.1	2.98

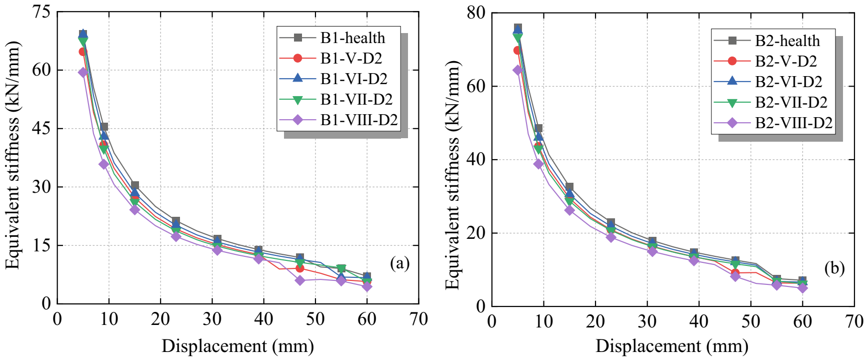

Fig. 62.9 The equivalent stiffness curves of shear wall B1 and B2 under different grouting defect combinations

the shear wall with grouting defects in the double-side concealed columns is higher than that of the single-side concealed columns. This may be V-D2 state makes the shear wall become an asymmetric member. The decrease rate of peak load F_p of shear wall B1 under different grouting defect combinations is 0.2–20.0%. The decrease rate of peak load F_p of shear wall B2 under different grouting defect combinations is 0.4–17.3%. The results show that with the increase of the concealed column width, the degree of weakening of the bearing capacity will be reduced.

It can be seen from Fig. 62.9 that the grouting defects of bilateral concealed columns have the greatest influence on the equivalent stiffness of shear wall. When there are grouting defects in the bilateral concealed columns, the equivalent stiffness of the shear wall B1-VIII-D2 decreases by 14.3%, and the equivalent stiffness of the shear wall B2-VIII-D2 decreases by 15.3%.

3. *Cumulative energy dissipation*. It can be seen from Fig. 62.10 that the energy dissipation capacity of shear wall B1 decreased by 20.9%, 2.1, 8.4 and 36.2% respectively under V-D2, VI-D2, VII-D2 and VIII-D2. Under the states of V-D2, VI-D2, VII-D2 and VIII-D2, the energy dissipation capacity of shear wall B2 decreased by 21.8, 3.8, 11.0 and 38.4% respectively. The results show that the influence of grouting defects on shear walls under different widths of concealed columns is close.

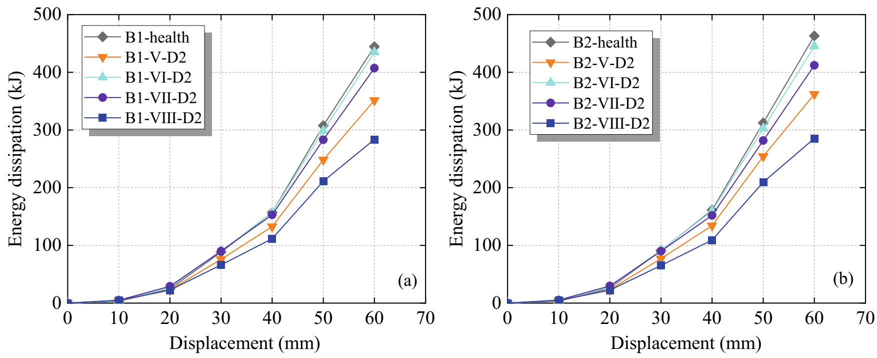

Fig. 62.10 The energy dissipation curves of shear wall B1 and B2 under different grouting defect combinations

62.4 Conclusion

In this paper, the seismic performance of concrete shear wall structure with sleeve grouting defects is analyzed. The influence of sleeve grouting defects on the seismic performance of shear wall with different design characteristics are studied. The main conclusions are as follows:

(1) Compared with the grouting-compact shear wall, the seismic performance of the grouting-defective shear wall will be reduced to different degrees, and the reduction degree of seismic performance parameters is positively correlated with the degree of grouting defect.
(2) Increasing the spacing of the sleeve distribution and the width of the concealed column in constraint zone is beneficial to improve the bearing capacity and ductility of the shear wall. However, in cyclic loading, increasing the spacing of the sleeve distribution and the width of the concealed column will lead to the early yield.
(3) The bearing capacity and energy dissipation capacity of the shear wall connected by grouting sleeve are greatly affected by grouting defects, and the equivalent stiffness and ductility coefficient are less affected by grouting defects than bearing capacity and energy dissipation capacity. The influence of grouting defects on the concealed column of the shear wall connected by grouting sleeve is more significant than that of the wall panel.

References

1. Xiao, S., et al.: Study of effects of sleeve grouting defects on the seismic performance of precast concrete shear walls. Eng. Struct. **236**, 111833 (2021)
2. Xu, F., et al.: Experimental bond behavior of deformed rebars in half-grouted sleeve connections with insufficient grouting defect. Constr. Build. Mater. **185**, 264–274 (2018)
3. Bahrami, S., et al.: Behavior of two new moment resisting precast beam to column connections subjected to lateral loading. Eng. Struct. **132**, 808–821 (2017)
4. Mirza, O., et al.: Behaviour of composite beam-column flush end-plate connections subjected to low-probability, high-consequence loading. Eng. Struct. **33**(2), 647–662 (2011)
5. Pan, G.B., et al.: An experimental study of the seismic behaviour of precast concrete shear walls with bolted-plate connections. Eng. Struct. **248**, 113203 (2021)
6. Xiong, E.G., et al.: Research on design and mechanical behavior of a new horizontal connection device of prefabri-cated shear wall. Constr. Build. Mater. **370**, 130713 (2023)
7. Ling, J.H., et al.: Feasibility study of grouted splice connector under tensile load. Constr. Build. Mater. **50**(1), 530–539 (2014)
8. Li, S.L., et al.: Influence of grouted sleeve and concrete strength of fabricated shear wall on acoustic emission detection method for sleeve compactness. J. Build. Eng. **43**, 102541 (2021)
9. Zhang, L., et al.: Characterization of damage progress in the defective grouted sleeve conection using combined acoustic emission and ultrasonics. Sensors **22**(21), 8579 (2022)
10. Wang, T., et al.: Evaluation of common defects of grouted sleeve connectors. Case Stud. Const. Mater. **17**, e01605 (2022)
11. Zheng, G.Y., et al.: Mechanical performance for defective and repaired grouted sleeve connections under uniaxial and cyclic loadings. Constr. Build. Mater. **233**, 117233 (2020)
12. Gu, S., et al.: Seismic performance of precast shear wall of insufficient grouting material strength strengthened with steel plate. Structures **45**, 1322–1332 (2022)
13. Mander, J.B., et al.: Theoretical stress-strain model for confined concrete. J. Struct. Eng. **114**(8), 1804–1825 (1988)
14. Lu, X.Z., et al.: A shear wall element for nonlinear seismic analysis of super-tall buildings using OpenSees. Finite Elem. Anal. Des. **98**, 14–25 (2015)
15. Cao, Z.J. et al.: Seismic fragility analysis of precast rc shear wall-frame structures with connection defects. 13th International Conference on Applications of Statistics and Probability in Civil Engineering. ICASP13, South Korea (2019)
16. JGJ355–2015: Technical specification for grout sleeve splicing of rebars. Beijing: Standards Press of China (2017)
17. JGJ3–2010: Technical specification for concrete structures of tall building. Beijing: China Building Industry Press (2010)